

# Time-series photometry of the O4 I(n)fp star $\zeta$ Puppis

Ian D. Howarth<sup>1\*</sup> and Ian R. Stevens<sup>2</sup>

<sup>1</sup>*Dept. Physics & Astronomy, University College London, Gower St., London WC1E 6BT*

<sup>2</sup>*School of Physics and Astronomy, University of Birmingham, Edgbaston, Birmingham B15 2TT*

16 October 2018

## ABSTRACT

We report a time-series analysis of the O4 I(n)fp star  $\zeta$  Pup, based on optical photometry obtained with the *SMEI* instrument on the *Coriolis* satellite, 2003–2006. A single astrophysical signal is found, with  $P = 1.780938 \pm 0.000093$  d and a mean semi-amplitude of  $6.9 \pm 0.3$  mmag. There is no evidence for persistent coherent signals with semi-amplitudes in excess of  $\sim 2$  mmag on any of the timescales previously reported in the literature. In particular, there is no evidence for a signature of the proposed rotation period,  $\sim 5.1$  days;  $\zeta$  Pup is therefore probably *not* an oblique magnetic rotator. The 1.8-day signal varies in amplitude by a factor  $\sim 2$  on timescales of 10–100d (and probably by more on longer timescales), and exhibits modest excursions in phase, but there is no evidence for systematic changes in period over the 1000-d span of our observations. Rotational modulation and stellar-wind variability appear to be unlikely candidates for the underlying mechanism; we suggest that the physical origin of the signal may be pulsation associated with low- $\ell$  oscillatory convection modes.

**Key words:** Asteroseismology, techniques: photometric, stars: oscillations, stars: individual:  $\zeta$  Pup

## 1 INTRODUCTION

There is no star in the sky that is both hotter and brighter than  $\zeta$  Pup (HD 66811; O4 I(n)fp,  $V = 2.24$ , Sota et al. 2011; Cousins 1972). As a result, it has long been a popular subject for the investigation of characteristics of massive, luminous stars in general, and of their radiatively driven stellar winds in particular, from both observational and theoretical perspectives (e.g. Lamers & Morton 1976; Barlow & Cohen 1977; De Loore et al. 1977; Snow et al. 1980; Abbott et al. 1980; Kudritzki et al. 1983; and many others subsequently).

### 1.1 Variability

One consequence of the scrutiny under which  $\zeta$  Pup has been placed is that there are numerous reports in the literature of low-level spectroscopic and photometric variability, across the electromagnetic spectrum. Although at least part of this variability appears to be stochastic, claims of periodic or cyclical signals can be grouped under three headings (cf. the summary in Table 1):

(i) *8.5-hour variability: non-radial pulsation?*

Baade (1986) discovered velocity-resolved structure in the photospheric absorption lines of  $\zeta$  Pup, with a possible 8.5-hr periodicity in data taken in 1984/5; Reid & Howarth

(1996) found very similar characteristics, with  $P = 8.54$  hr, in spectra taken in 1990.

The observations show characteristic blue-to-red migration of bumps and dips in the absorption-line profiles, suggesting non-radial pulsation as the underlying physical mechanism; a tentative identification of a sectoral mode with  $\ell = -m = 2$  has been proposed (Baade 1988; Reid & Howarth 1996).

However, while the general nature of the line-profile variability persisted in spectra taken in 1986 and 2000, the periodic signal could not be recovered in those data (Baade 1991; Donati & Howarth, unpublished), showing it to be transient, or variable in amplitude.

(ii) *17–19-hr variability: recurrent wind structures?*

Unsaturated P-Cygni profiles of UV resonance lines in OB stars commonly show ‘discrete absorption components’ (DACs; e.g., Prinja & Howarth 1986; Kaper et al. 1999), which migrate bluewards through the absorption troughs. Howarth et al. (1995) found a DAC recurrence timescale of 19 hours in 16 days of IUE observations of  $\zeta$  Pup taken in 1995. Essentially the same period was recovered from observations of  $H\alpha$  (a wind-formed line for  $\zeta$  Pup) taken in 1990 (Reid & Howarth 1996), while Prinja et al. (1992) suggested a DAC recurrence timescale of around 15 hr, though from only two days of intensive IUE observations in 1989.

X-ray emission from hot stars arises in shocked material in their stellar winds, and so is another tracer of the outflows. Berghöfer et al. (1996) reported a low-amplitude 17-hr

\* i.howarth@ucl.ac.uk

**Table 1.** Summary of periods reported for  $\zeta$  Pup. ‘DACs’ refers to discrete absorption components in the absorption troughs of UV P-Cygni profiles, while ‘lpv’ means (photospheric) line-profile variability.

Period	Epoch	Source	
$5.075 \pm 0.003$ d	1975–1976	Moffat & Michaud (1981)	H $\alpha$ absorption
$\sim 5.26$ d	1986	Balona (1992)	Photometry
$5.21 \pm 0.71$ d	1995	Howarth et al. (1995)	DACs
$\sim 15$ h	1989	Prinja et al. (1992)	DACs
$19.23 \pm 0.45$ h	1995	Howarth et al. (1995)	DACs
$19.57 \pm 0.48$ h	1990	Reid & Howarth (1996)	H $\alpha$ variability
$16.67 \pm 0.81$ h	1991	Berghöfer et al. (1996)	0.1–2.4keV
$16.90 \pm 0.48$ h	1991	Berghöfer et al. (1996)	H $\alpha$ variability
$\sim 8.5$ h	1984	Baade (1986)	lpv
$8.54 \pm 0.054$ h	1990	Reid & Howarth (1996)	lpv
$1.780938 \pm 0.000093$ d	2003–2006	This paper	Photometry

signal in 11 days’ of ROSAT data, 0.9–2 keV (undetectable at lower energies), obtained in 1991 October. Although this signal is not of itself particularly persuasive (cf. the discussion in Nazé et al. 2013), eight days (*sic*) of contemporaneous H $\alpha$  spectroscopy reported by Berghöfer et al. (1996) showed the same  $\sim$ periodic signature. However, Nazé et al. (2013) analysed a larger, XMM-Newton, dataset (16 separate observations, 2002–2010) and found no periodic signals, concluding that “variations of several hours and an amplitude of a few per cent. . . is transient, at best.”

It seems plausible that all these signals may reflect a single loose, and possibly transitory, timescale in the stellar wind. Berghöfer et al. (1996) pointed out that this timescale is ca.  $2\times$  the period found from the absorption-line profiles, but concluded that there is no obvious physical connection.

### (iii) 5.1-d variability: rotation?

Moffat & Michaud (1981) detected a modulation in the absorption component of the H $\alpha$  P-Cygni profile in 1975–1976, consistent with a 5.1-day period. They interpreted this as the stellar rotation period, suggesting that the inner regions of the stellar wind are forced into co-rotation by a magnetic field; that is, that  $\zeta$  Pup is an oblique magnetic rotator. Balona (1992) found a marginal signal with a semi-amplitude of  $\sim 0.01$  at  $P \simeq 5.2$  d in Strömgren *b* photometry from 1986, but not from 1989; he also noted that the dispersion in the photometry was much larger than the internal errors, concluding that  $\zeta$  Pup is an irregular microvariable.

Howarth et al. (1995) reported a similar period in UV data ( $P = 5.2$  d), although this is close to the  $1 \text{ d}^{-1}$  alias of the 19-hr signal found in the same dataset; and Baade (1986) made the interesting observation that measurements of H $\alpha$  variability reported by Moffat & Michaud (1981) give a stronger signal at the mooted NRP period of 8.5 h than the Moffat & Michaud period of 5.1 d in a phase-dispersion-minimization periodogram (though they recognized that the shorter period is far below the Nyquist period of the data).

While the evidence for each of these three variability timescales is reasonable, in every case it falls short of providing a compelling demonstration of a persistent, coherent signal, in large part because of the observational difficulties in obtaining extensive, well-sampled time series with appropriate duration and cadence on a very bright target. A robust determination of the supposed rotation period would be

of particular value, not only because of the intrinsic interest of testing the proposed oblique rotator model, but also because, coupled with the observed  $v_e \sin i$ , it would provide a strong constraint on the stellar radius, and hence the distance, which is poorly known (Section 3).

## 2 TIME-SERIES ANALYSIS

### 2.1 Observations

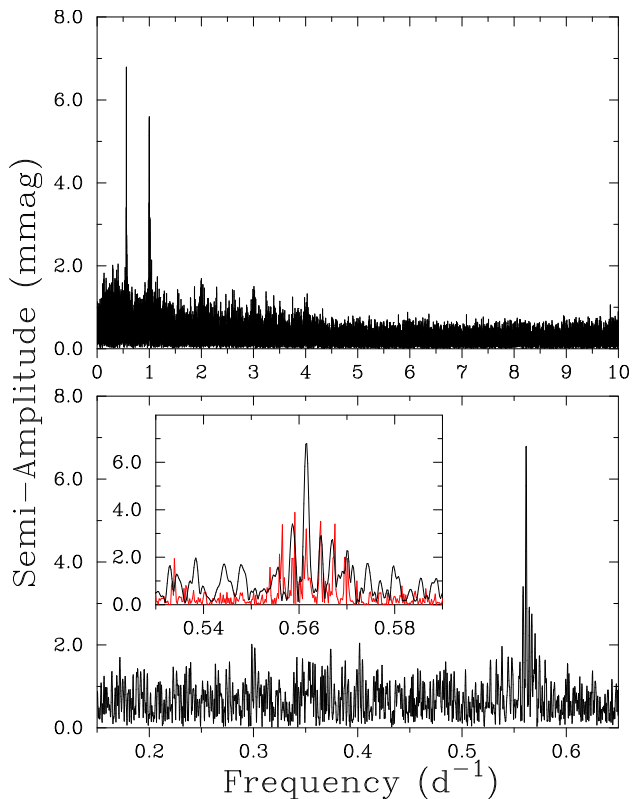
With the foregoing in mind, we have undertaken a time-series analysis of  $\zeta$  Pup photometry obtained with the Solar Mass Ejection Imager, *SMEI*. This was one of two instruments on the *Coriolis* satellite, and incorporated three imaging cameras; here we only use results from cameras 1 and 2, which have the best data quality, spanning 1077 d, grouped into four seasonal runs of 40, 236, 211, and 175 days (2003 April to 2006 March), with a median cadence of 101 minutes. The passband was dominated by the CCD detector response, peaking at 45 per cent at 700 nm, and falling to 10 per cent at  $\sim 460$  and 990 nm. Further details on the *SMEI* instrument and data-handling pipeline can be found in Eyles et al. (2003) and Spreckley & Stevens (2008).

All *SMEI* photometry shows long-term variations of instrumental origin (e.g., Goss et al. 2011), which we removed with a ten-day running-mean filter.<sup>1</sup> The trend-corrected observations have a dispersion characterized by  $\sigma = 19.4$  mmag; we analysed both the full dataset, and a subset with a  $3\text{-}\sigma$  clip applied (6918 and 6855 measurements, respectively), obtaining essentially identical results. Numerical values reported here are based on the clipped subset.

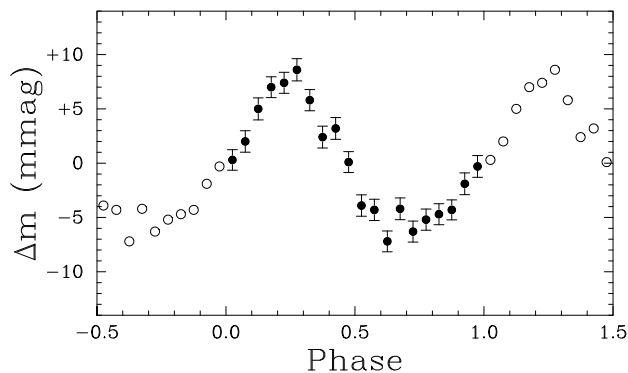
### 2.2 Global data properties

Fig. 1 shows the date-compensated discrete component fourier transform of the entire dataset, over the frequency range  $0\text{--}10 \text{ d}^{-1}$  (DCDFT; Ferraz-Mello 1981); the Nyquist frequency is at  $7.086 \text{ d}^{-1}$ . There is a single clear astrophysical signal (in addition to an instrumental signal at  $1 \text{ d}^{-1}$  and multiples thereof), with

<sup>1</sup> We performed simulations to verify that this has no significant impact on our sensitivity to  $\sim 5$ -d signals.



**Figure 1.** Date-compensated discrete Fourier transform of  $\zeta$  Pup photometry. The inset in the lower panel shows the region of the  $0.56\text{-d}^{-1}$  signal, overlaid with a shifted version of the window function (in red).



**Figure 2.** Photometry binned at  $P = 1.78$  d (arbitrary phasing)

$$\nu = 0.561502 (29) \text{ d}^{-1} \quad [P = 1.780938 (93) \text{ d}],$$

$$\text{semi-amplitude} = 6.69 (31) \text{ mmag},$$

where bracketed values are  $1\text{-}\sigma$  uncertainties in the last significant figures, generated by 10 000 Monte-Carlo replications of artificial datasets having the same input signal plus gaussian noise (and are slightly larger than the formal single-parameter errors from a least-squares fit of a sinusoid). A minor periodogram peak occurs at the first harmonic (semi-amplitude  $1.6$  mmag at  $\nu = 1.123$   $\text{d}^{-1}$ ); although this would not be significant in isolation, there is  $<0.1\%$  probability that a peak this strong should appear at this particular frequency by chance. Fig. 2 shows the phased, binned data, and confirms that the signal is only slightly non-sinusoidal.

There is *no* convincing signature of the mooted  $\sim 5\text{-d}$  rotation period. The mean semi-amplitude in the DCDFT over the frequency range  $0\text{--}0.5$   $\text{d}^{-1}$  is  $0.66 \pm 0.37$  mmag (s.d.); the corresponding figures over the  $0.18\text{--}0.21$   $\text{d}^{-1}$  range are essentially indistinguishable ( $0.66 \pm 0.36$  mmag). There are several peaks in the latter range with semi-amplitudes up to  $1.3\text{--}1.4$  mmag (which are entirely unremarkable in the context of the broader frequency range); the strongest, at  $\nu = 0.1952$   $\text{d}^{-1}$ , has a semi-amplitude of  $1.4 \pm 0.3$  mmag.<sup>2</sup> We would not expect any significant change in period, or phase, of a truly rotationally modulated signal over the course of our observations, so our interpretation of these results is that there is a  $3\text{-}\sigma$  upper limit of  $2.3$  mmag on the semi-amplitude of any such signal in the period range  $P = 4.8\text{--}5.5$  d.

### 2.3 Transitory signals

The global DCDFT is primarily sensitive to signals at fixed phase and period; cancellation will occur for signals which recur with different phasing, or which drift in frequency – circumstances that might well be expected to apply to the  $\sim 8.5\text{-hr}$  and  $\sim 17\text{-hr}$  signals discussed in Section 1. We therefore computed DCDFTs for seasonal subsets of the data, and for 50-day sequences (starting every 25 days). There is no suggestion of significant power at either of the shorter periods, at any time.

The same subsets allow us to examine the coherence and stability of the  $1.78\text{-d}$  signal. The semi-amplitudes and periods are summarized in Fig. 3 (top two panels), where the error bars were generated analytically following Montgomery & O’Donoghue (1999). Because the points are not independent, and because the analytical error estimates are rigorous only under restricted conditions, we investigated the probability that the null hypotheses of constant frequency and constant semi-amplitude can be ruled out by using a simple Monte-Carlo approach, utilising the fact that the dispersion in the observations is dominated by observational errors (and not by the periodic signal).

To do this, we took the original dataset and, with observing dates fixed, shuffled the flux values (using the Fisher-Yates algorithm; we verified that this removed all periodic signals). We then planted an artificial, periodic signal with characteristics matching those found in the original data, and analysed the results in an identical fashion.

We find that 13% of 10 000 replications result in  $\chi^2$  values as large or larger than that actually obtained for the frequencies, but that none of the simulations result in a  $\chi^2$  value for the amplitudes as large as that found in the data. We conclude that this test provides no evidence for changes in period, but that the amplitude of the photometric signal varies, by a factor  $\sim 2$  in our data.

Because the semi-amplitude found for the entire dataset is consistent with the mean of the subset semi-amplitudes, it is unlikely that there is significant phase slippage during our observations (which would dilute the signal in the full dataset). We examined the coherence of the  $1.78\text{-d}$  signal by determining the phase, for fixed period, in the subsets

<sup>2</sup> Of course, this doesn’t represent a ‘ $3\text{-}\sigma$  detection’, because we have selected this frequency *a posteriori* from the several thousand independent frequencies available.

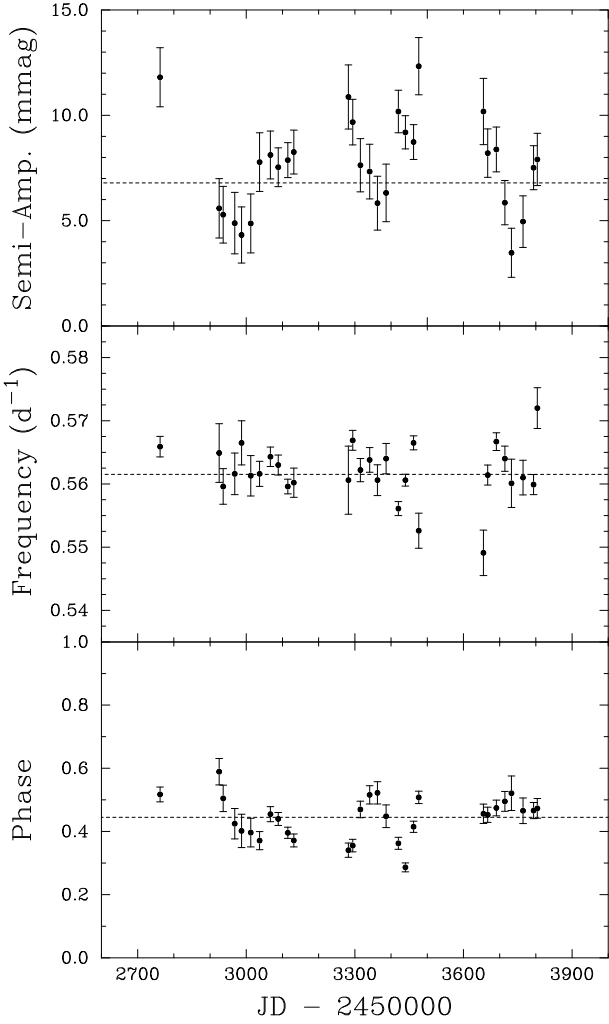


**Figure 3.** Top two panels: semi-amplitudes and frequencies for the  $0.56 \text{ d}^{-1}$  signal from 50-d subsets of the data, sampled every 25 d. Mean values from the global analysis are shown by horizontal lines. Bottom panel: phase of the 1.78-d signal (referenced to midpoint of the times series), with error bars computed analytically (cf. Section 2.3).

(Fig. 3, bottom panel). Monte-Carlo simulations show that the phase ‘wander’ seen in Fig. 3, while of fairly low amplitude, is too large to have arisen by chance, with  $> 99.9\%$  confidence.

### 3 DISCUSSION

The discovery of a strong, periodic signal in such a well-studied star is superficially surprising, but may in part be a consequence of  $\zeta$  Pup being too bright for many programmes, and of the period being too long to identify in short data streams. Moreover, although the signal was consistently present, and remained essentially coherent, over the three years of our dataset, it isn’t necessarily a permanent feature. Had the signal reported here been present with a comparable amplitude in 1986–89, the time of the observations discussed by Balona (1992), it would certainly have been detected (Balona, personal communication).

Physical interpretation of the signal is handicapped

**Table 2.** Stellar parameters, from Bouret et al. (2012; B12) and Pauldrach et al. (2012; P12).  $P_{\min}$  is the minimum rotation period (§3.1), and  $Q$  the pulsation ‘constant’ (§3.4). Bracketed values in italics are rescaled to distances  $d = [332, 540]$  pc (cf. §3); mass-loss rates are scaled assuming  $\dot{M} \propto d^{3/2}$ .

Parameter	B12	P12
$T_{\text{eff}}$ (kK)	40.0	40.0
$\log g$ (dex cgs)	3.64	3.40
$v_e \sin i$ (km s $^{-1}$ )	210	220
$v_{\infty}$ (km s $^{-1}$ )	2300	2100
Adopted $d$ (pc)	460	692
$-\log \dot{M}$ (dex $M_{\odot} \text{yr}^{-1}$ )	5.70	4.86
	<i>[5.91, 5.60]</i>	<i>[5.34, 5.02]</i>
$R/R_{\odot}$	18.8	28.0
	<i>[13.6, 22.1]</i>	<i>[13.4, 21.8]</i>
$\log(L/L_{\odot})$	5.91	6.26
	<i>[5.63, 6.05]</i>	<i>[5.62, 6.04]</i>
$M/M_{\odot}$	56	72
	<i>[29, 78]</i>	<i>[17, 44]</i>
$P_{\text{rot}}/\sin i$ (d)	4.5	6.4
	<i>[3.3, 5.3]</i>	<i>[3.1, 5.0]</i>
$P_{\min}$ (d)	2.1	3.4
	<i>[1.8, 2.3]</i>	<i>[2.3, 3.0]</i>
$Q$ (d)	0.16	0.10
	<i>[0.19, 0.15]</i>	<i>[0.15, 0.12]</i>

by uncertainties in many of  $\zeta$  Pup’s fundamental parameters, which are a direct consequence of the uncertainty in its distance. Although the *Hipparcos* parallax yields  $d = 332 \pm 11$  pc (van Leeuwen 2007; see also Schilbach & Röser 2008, Maíz Apellániz et al. 2008), this leads to estimates of the stellar mass that are substantially smaller than generally accepted values for O supergiants (Bouret et al. 2012), and a case can be made for  $d \simeq 700$  pc (e.g., Pauldrach et al. 2012). Furthermore, *if* the stellar rotation period were  $P_{\text{rot}} \simeq 5.1$  d, then the equatorial rotation speed<sup>3</sup> of  $v_e \simeq 220 \text{ km s}^{-1}$  would imply  $R \simeq 22R_{\odot}$ , whence  $d \simeq 540$  pc.

Consequently, while parameters that can be determined directly from the spectrum are reasonably well established (e.g.,  $T_{\text{eff}}$ ,  $\log g$ ,  $v_{\infty}$ ), the mass, radius, and luminosity are more poorly known; the mass-loss rate has additional uncertainties arising from clumping in the wind. For reference, results from two recent analyses, obtained using independent state-of-the-art modelling tools, are summarized in Table 2, along with ancillary distance-dependent derived quantities.

#### 3.1 Rotation

For a Roche model, the minimum possible stellar rotation period for a positive equatorial effective gravity is

$$P_{\min} = 3\pi\sqrt{R_{\text{eq}}/g_{\text{p}}},$$

where  $R_{\text{eq}}$  is the equatorial radius and  $g_{\text{p}}$  is the polar gravity. We include estimates of  $P_{\min}$  in Table 2, taking  $g_{\text{p}} = g$  and  $R_{\text{eq}} = \sqrt{1.5}R$ .

Estimates of the maximum rotation period,  $P_{\text{rot}}/\sin i$

<sup>3</sup> Since  $\zeta$  Pup has one of the largest known  $v_e \sin i$  values among the O supergiants (e.g., Howarth et al. 1997), it is likely that  $\sin i \simeq 1$ .

(which is probably close to the true rotation period), follow from  $v_e \sin i$  and  $R$ ; these are also reported in Table 2.

The 1.78-d photometric signal is only marginally consistent with the shortest possible rotation period, and is substantially shorter than any plausible estimate of the true rotation period. Eschewing numerological speculation (e.g.,  $P_{\text{rot}} \simeq 3P_{\text{phot}}?$ ), this appears to rule out rotational modulation as the cause of the photometric variability.

### 3.2 Wind variability

The optical depth through the wind can be estimated by integrating the equation of mass continuity for an assumed ‘beta’ velocity law,

$$v(r) = v_\infty(1 - R_*/r)^\beta.$$

The result is mildly sensitive to the adopted  $\beta$  index, and to  $v_0$ , the minimum velocity used for the integration, but, for  $0.6 \leq \beta \leq 1.2$ ,  $15 \leq (v_0/\text{km s}^{-1}) \leq 30$ , the electron-scattering optical depth is within a factor  $\sqrt{3}$  of

$$\tau_{\text{es}} \simeq 0.08 \times \left[ \frac{\dot{M}/(M_\odot \text{ yr}^{-1})}{3.5 \times 10^{-6}} \right] \left[ \frac{R_*/R_\odot}{18.8} \frac{v_\infty/(\text{km s}^{-1})}{2200} \right]^{-1},$$

where we have used the mass-loss rate from Cohen et al. (2010), for their adopted distance of 460 pc; the radius is scaled to the same distance. (The numerical values of both  $R_*$  and this  $\dot{M}$  are directly proportional to  $d$ , so their ratio is distance-independent.)

The photometric variability, if attributed to changes in continuum optical depth of the stellar wind, would require  $\Delta\tau \simeq 0.013$ ; that is, the wind column would have to vary by 15–20%. While not out of the question, such a large, periodic modulation is unlikely to have escaped notice in previous dedicated stellar-wind studies, and would require a driving mechanism independent of rotation.

### 3.3 Magnetic confinement

The absence of a detectable rotational signature at the Mofat & Michaud (1981) 5.1-d period is noteworthy. Their result was based only 35 points, and they note that different amplitudes, and slightly different best-fitting periods, pertain to two different observing seasons, so the case for a strictly rotationally modulated signal is not compelling, and rests largely on the near-coincidence with estimates of the rotation period based on  $v_e \sin i$  (Table 2).

For  $\tau_{\text{es}} \simeq 0.1$ , an upper limit of  $\sim 5$  mmag on rotational photometric variability implies a column-density modulation  $\lesssim 5\%$  in an asymmetric wind. Thus if  $\zeta$  Pup is indeed an oblique magnetic rotator, then  $B_p$ , the dipole field strength at the magnetic pole, is insufficient to shape the wind significantly. Following ud-Doula & Owocki (2002), this implies

$$B_p \lesssim 100 \left[ \frac{\dot{M}/(M_\odot \text{ yr}^{-1})}{3.5 \times 10^{-6}} \frac{v_\infty/(\text{km s}^{-1})}{2200} \right]^{1/2} \left[ \frac{18.8}{R_*/R_\odot} \right] \text{G}.$$

[As this paper was being prepared for submission, David-Uraz et al. (2014) reported a 95-% confidence upper limit on a dipolar field strength of  $B_p < 121$  G, based on one night’s spectropolarimetric observations, consistent with our result.]

### 3.4 Pulsation

Pulsation would seem to be a plausible candidate mechanism for generating the photometric signal. We include estimates of the pulsation ‘constant’,<sup>4</sup>

$$Q = P\sqrt{(M/M_\odot)/(R/R_\odot)^3}$$

in Table 2, finding  $Q \simeq 0.1\text{--}0.2$  d.

Zeta Pup is expected to be unstable to low-order (radial)  $p$ -mode oscillations according to Saio (2011); the luminosity:mass ratio,  $\sim 4.3 \pm 0.1$  ( $\log_{10}$  solar units), is large enough to suggest the strange-mode instability associated with the iron-opacity peak as the driving mechanism. However, expected  $Q$  values are  $\sim 0.03$  d, substantially smaller than observed.

The 1.8-d period is therefore more likely to be associated with the oscillatory convection modes discussed by Saio (2011). The  $Q$  values for low-order ( $\ell = 1, 2$ ) modes, which are expected to be the most readily observable, are  $\sim 0.2\text{--}0.3$  for the models most likely to be relevant to  $\zeta$  Pup<sup>5</sup> (core hydrogen burning, solar metallicity,  $M_{\text{ZAMS}} \simeq 60 M_\odot$ ), reasonably consistent with our observed value.

We arrive at this conclusion in part through the application of Holmes’ maxim (Doyle 1892, p. 524), as the match in  $Q$  is far from perfect, and the inclusion of rotation in the models is liable to shift the predicted frequencies to larger values. Furthermore, in displaying a single, strong signal, the frequency spectrum for  $\zeta$  Pup differs from those found for other early-type O stars, which appear to have power spectra dominated by red noise (Blomme et al. 2011), although the available sample is small. We speculate that a range of modes may actually be excited in  $\zeta$  Pup, and that we have seen just the ‘tip of the iceberg’.

## 4 SUMMARY

Four years’ of  $\zeta$  Pup photometry from the *SMEI* instrument, 2003–6, reveals a single astrophysical signal, with  $P = 1.780938 \pm 0.000093$  d and a mean semi-amplitude of  $6.9 \pm 0.3$  mmag. The period appears too short to be rotational, and the amplitude too large to arise through wind variability. We therefore tentatively attribute the signal to

<sup>4</sup> Osborn’s law: variables won’t, constants aren’t.

<sup>5</sup> Saio (personal communication) points out that  $Q \simeq 0.06\text{--}0.08$  for Geneva models with initial masses  $\sim 40\text{--}50M_\odot$  during core helium burning, when they return to the vicinity of the main sequence following an excursion to the red in the Hertzsprung-Russell diagram. In principle, this could be consistent our results, particularly since the models predict masses at this stage that are  $\sim$ half the zero-age main-sequence values, with a commensurate reduction in the ‘observed’  $Q$ . However, although it is generally accepted that CNO-processed material is exposed at the surface of  $\zeta$  Pup (e.g., Bouret et al. 2012), surface abundances have not progressed to the strongly non-solar values predicted at this stage in evolutionary models by, e.g., Ekström et al. (2012). Moreover, single-star evolutionary models show considerable rotational spindown over the main-sequence phase; the exceptionally high  $v_e \sin i$  observed for  $\zeta$  Pup therefore argues for it being core hydrogen burning. Merger models offer an alternative mechanism for generating rapid rotation, but core hydrogen burning appears to be in effect even for the merger model discussed by Pauldrach et al. (2012).

pulsation, possibly associated with low-order oscillatory convection modes. Any signal associated with a mooted  $\sim 5$ -d rotation period had a semi-amplitude  $< 2.3$  mmag at the time of our observations, with  $3\text{-}\sigma$  confidence.

## ACKNOWLEDGEMENTS

We thank Hideyuki Saio for suggestions, Vino Sangaralingam for assistance with initial data processing, and our referee, Luis Balona, for helpful remarks.

## REFERENCES

- Abbott D. C., Biegging J. H., Churchwell E., Cassinelli J. P., 1980, *ApJ*, 238, 196
- Baade D., 1986, in Gough D. O., ed., *NATO ASIC Proc. 169: Seismology of the Sun and the Distant Stars*, pp 465–466
- Baade D., 1988, *NASA Special Publication*, 497, 137
- Baade D., 1991, in Baade D., ed., *Rapid Variability of OB-Stars: Nature and Diagnostic Value*, Vol. 36 of *European Southern Observatory Conference and Workshop Proceedings*. p. 21
- Balona L. A., 1992, *MNRAS*, 254, 404
- Barlow M. J., Cohen M., 1977, *ApJ*, 213, 737
- Berghöfer T. W., Baade D., Schmitt J. H. M. M., Kudritzki R.-P., Puls J., Hillier D. J., Pauldrach A. W. A., 1996, *A&A*, 306, 899
- Blomme R., Mahy L., Catala C., Cuypers J., Gosset E., Godart M., Montalban J., Ventura P., Rauw G., Morel T., Degroote P., Aerts C., Noels A., Michel E., Baudin F., Baglin A., Auvergne M., Samadi R., 2011, *A&A*, 533, A4
- Bouret J.-C., Hillier D. J., Lanz T., Fullerton A. W., 2012, *A&A*, 544, A67
- Cohen D. H., Leutenegger M. A., Wollman E. E., Zsargó J., Hillier D. J., Townsend R. H. D., Owocki S. P., 2010, *MNRAS*, 405, 2391
- Cousins A. W. J., 1972, *Monthly Notes of the Astronomical Society of South Africa*, 31, 69
- David-Uraz A., Wade G. A., Petit V., ud-Doula A., Sundqvist J. O., Grunhut J., Shultz M., Neiner C., Alecian E., Henrichs H. F., Bouret J.-C., and the MiMeS Collaboration 2014, *MNRAS*, in press (arXiv 1407.6417)
- De Loore C., De Greve J. P., Lamers H. J. G. L. M., 1977, *A&A*, 61, 251
- Doyle A. C., 1892, *The Strand Magazine*, 3, 511
- Ekström S., Georgy C., Eggenberger P., Meynet G., Mowlavi N., Wyttenbach A., Granada A., Decressin T., Hirschi R., Frischknecht U., Charbonnel C., Maeder A., 2012, *A&A*, 537, A146
- Eyles C. J., Simnett G. M., Cooke M. P., Jackson B. V., Buffington A., Hick P. P., Waltham N. R., King J. M., Anderson P. A., Holladay P. E., 2003, *Solar Physics*, 217, 319
- Ferraz-Mello S., 1981, *AJ*, 86, 619
- Goss K. J. F., Karoff C., Chaplin W. J., Elsworth Y., Stevens I. R., 2011, *MNRAS*, 411, 162
- Howarth I. D., Prinja R. K., Massa D., 1995, *ApJL*, 452, L65
- Howarth I. D., Siebert K. W., Hussain G. A. J., Prinja R. K., 1997, *MNRAS*, 284, 265
- Kaper L., Henrichs H. F., Nichols J. S., Telting J. H., 1999, *A&A*, 344, 231
- Kudritzki R. P., Simon K. P., Hamann W.-R., 1983, *A&A*, 118, 245
- Lamers H. J. G. L. M., Morton D. C., 1976, *ApJS*, 32, 715
- Maíz Apellániz J., Alfaro E. J., Sota A., 2008, *ArXiv* 0804.2553
- Moffat A. F. J., Michaud G., 1981, *ApJ*, 251, 133
- Montgomery M. H., O’Donoghue D., 1999, *Delta Scuti Star Newsletter*, 13, 28
- Nazé Y., Oskinova L. M., Gosset E., 2013, *ApJ*, 763, 143
- Pauldrach A. W. A., Vanbeveren D., Hoffmann T. L., 2012, *A&A*, 538, A75
- Prinja R. K., Balona L. A., Bolton C. T., Crowe R. A., Fieldus M. S., Fullerton A. W., Gies D. R., Howarth I. D., McDavid D., Reid A. H. N., 1992, *ApJ*, 390, 266
- Prinja R. K., Howarth I. D., 1986, *ApJS*, 61, 357
- Reid A. H. N., Howarth I. D., 1996, *A&A*, 311, 616
- Saio H., 2011, *MNRAS*, 412, 1814
- Schilbach E., Röser S., 2008, *A&A*, 489, 105
- Snow Jr. T. P., Kunasz P. B., Wegner G. A., 1980, *ApJ*, 238, 643
- Sota A., Maíz Apellániz J., Walborn N. R., Alfaro E. J., Barbá R. H., Morrell N. I., Gamen R. C., Arias J. I., 2011, *ApJS*, 193, 24
- Spreckley S. A., Stevens I. R., 2008, *MNRAS*, 388, 1239
- ud-Doula A., Owocki S. P., 2002, *ApJ*, 576, 413
- van Leeuwen F., 2007, *A&A*, 474, 653